RUMBLING IN HIGH SPEED PASSENGER TRAINS

M. M E Y W E R K   (BRAUNSCHWEIG)

A model of a flexible wheel set running on flexible rails is presented. It gives hints for the reasons of rumbling in the high-speed passenger train InterCityExpress (ICE) of the German railway company (DB) if these trains travel on the new stiff tracks. The rumbling results from non-circular wheels which cause oscillations of the whole system. The problem of polygonization of railway wheels is not considered.

1. INTRODUCTION

The 100 Hz-rumbling of the German high-speed train ICE in the passenger coaches diminishes the travel comfort. An investigation of the excitation mechanism is necessary to understand the problem and to avoid this noise. The characteristics of the rumbling are as follows:

1. The frequency of the rumbling is in the range of 90 Hz to 110 Hz, nearly independent of the train velocity.

2. The rumbling spectrum shows higher harmonics of the revolutions (or the mean angular velocity Ω) of the wheel sets.

3. The rumbling noise increases with increasing non-circularity of the wheels.

4. The rumbling occurs mainly on the new, stiff tracks of DB.

2. THE MODEL

We assume that the non-circular profiles of the wheels are periodic functions of φ, the azimuthal variable. These non-circularities produce oscillations of the whole system consisting of the coach and the track. We consider here only a part of the system which is sketched in Fig. 1. It consists of the rails and one wheel set which is guided by the wheel frame (since in our model the wheel frame can not rotate, we prefer this name instead of bogie). The wheel frame moves with constant velocity v in $\vec{e}_{g1}$-direction. The wheel frame and the wheel set are joined by three spring-damper pairs (not sketched in Fig. 1) at each end of the axle.

The rails, the rims of the wheels, and the axle are described in the model as one-dimensional continua; the wheel disks by two-dimensional continua. We call a flexible body an n-dimensional continuum (n being a natural number) if the deflection(s) depend(s) on n independent spatial variables. The hubs are assumed to be rigid bodies. We assume a linear viscoelastic law for the stress-strain relation, i.e. $\sigma_{ij} = E_{ij}^{kl} (1 + \eta \partial/\partial t) \varepsilon_{kl}$ where E_{ij}^{kl} is the tensor of elasticity and η is the so-called relaxation time (cf. FUNG [1], p. 24).
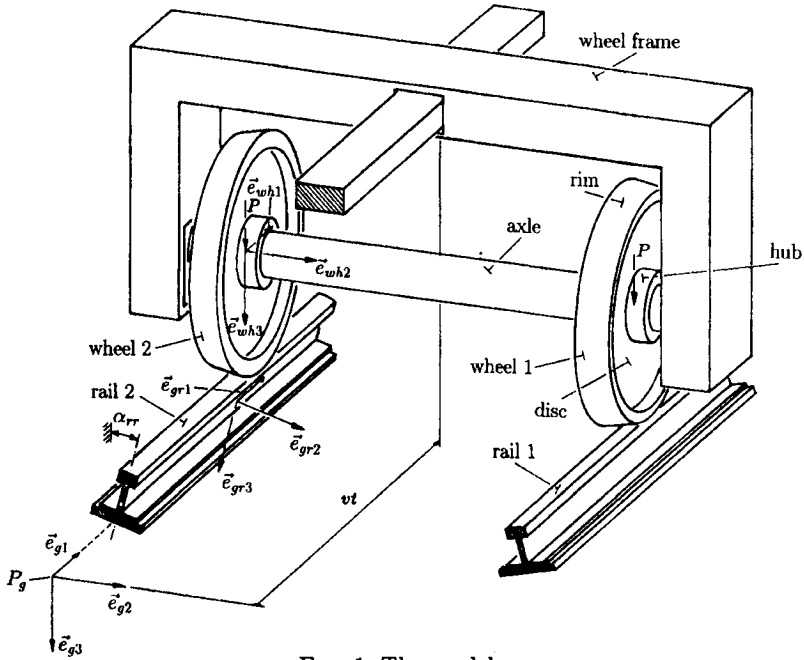

FIG. 1. The model.

The deflections u_{wa} and w_{wa} of the axle and the angles of rotation α_{wa}, γ_{wa} of the cross-section in $\vec{e}_{g1}$- and $\vec{e}_{g3}$- direction (cf. Fig. 2, $\vec{e}_{g1} = \vec{e}_{wa1}$, $\vec{e}_{g3} = \vec{e}_{wa3}$), respectively, are governed by two systems of partial differential equations of Timoshenko beams. Due to the rotation of the axle, the two systems are coupled (cf. WAUER [11]). For the deflection v_{wa} and the angle of rotation β_{wa} of the axle we choose the partial differential equations of a bar subject to extension and torsion (cf. PILKEY [8], p. 593). The functions u_{wa}, v_{wa}, w_{wa}, α_{wa}, β_{wa}, and γ_{wa} depend on the spatial coordinate y in the $\vec{e}_{wa2}$-direction and the time t.

We describe the degrees of freedom for the wheels and the rails, e.g. for wheel 1 and rail 1 and drop the index 1. The hub has six degrees of freedom: three for translation u_{wh}, v_{wh}, w_{wh} and three for rotation α_{wh}, β_{wh} γ_{wh} (cf. Fig. 3). The deflections of the hubs and those of the axle at its ends are coupled by geometrical and mechanical boundary conditions.
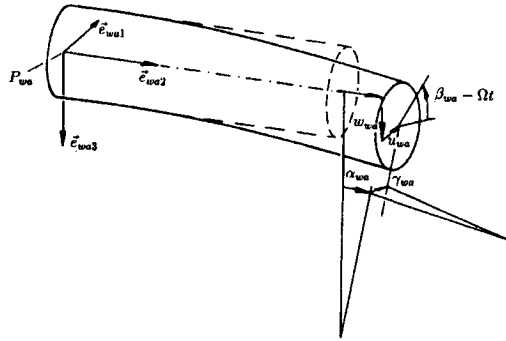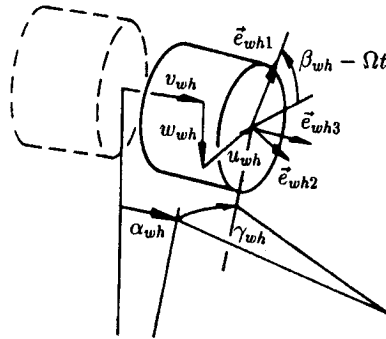
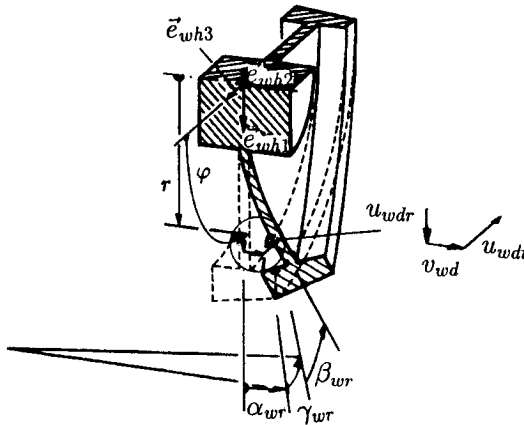FIG. 2. Deflections of the axle.

FIG. 3. Degrees of freedom of hub 1.

FIG. 4. Deflections of disk 1.

[317]

We assume that the wheel disk is clamped at the hub. Kirchhoff's plate theory governs the deflection v_{wd} of the disk perpendicular to its middle plane (cf. Fig. 4). The deflections u_{wdr}, u_{wdt} in the middle plane are governed by the equations of a shell (cf. WASHIZU [10], p. 159). The functions v_{wd}, u_{wdr}, u_{wdt} depend on the azimuthal angle φ, the radial coordinate r, and time t.

The partial differential equations of a Timoshenko beam and a bar in torsion and extension describe the motions of the rim. There is one additional degree of freedom for each rim. This is the rotation β_{wr} of the cross-sections with respect to the $\vec{e}_{wh2}$ direction ($\vec{e}_{wh}$ is the local coordinate system fixed to the hub). The equations of motion of the rim are obtained by following the way outlined by TEICHMANN [9].

The deflections v_r and w_r of the rail in $\vec{e}_{g2}$- and $\vec{e}_{g3}$-direction, respectively, obey the partial differential equations of a Timoshenko beam. The corresponding angles are γ_r and β_r (cf. Fig. 5). The deflections u_r and the rotation α_r are governed by the equations of a bar in extension and torsion, respectively. The deflections u_r, v_r, w_r and the angles α_r, β_r, γ_r depend on the spatial coordinate $s := x - vt - u_{cr}$ (moving coordinate system; the point of contact is located on the cross-section Q_{cr} whose position is given by u_{cr}, cf. Fig. 5), and on time t.
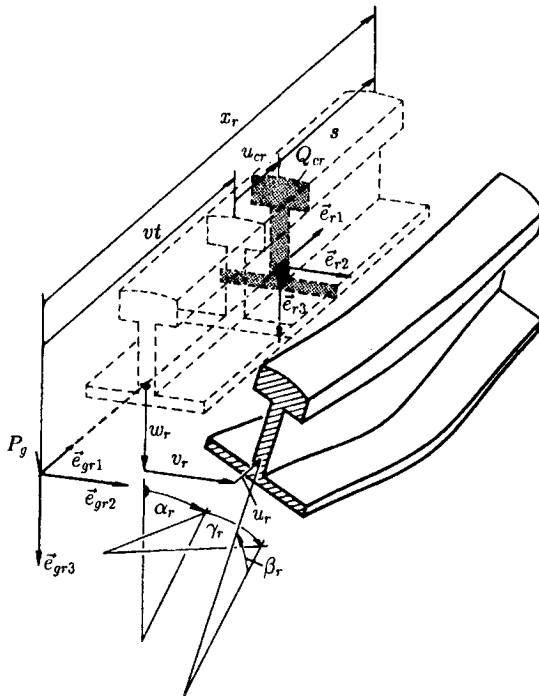

FIG. 5. Deflections of rail 1.

The wheels and the respective rails are coupled via Kalker's linear contact theory (cf. KALKER [2]), the linearized Hertzian contact stiffnesses, geometrical and mechanical boundary conditions, and equations which describe the smoothness of the wheels and the rails at the points of contact. We call these equations the contact equations.

The resulting set of equations is linear, homogeneous, autonomous and it consists of partial and ordinary differential equations and algebraic equations.

The equations of motion are derived by the principle of Hamilton-Ostrogradskij:

$$(2.1) \qquad 0 = \tilde{\delta} S = \int_{t=t_1}^{t_2} (\delta T - \delta U + \tilde{\delta} W) \, dt \ .$$

Here δT is the variation of the kinetic energy, δU is the variation of the potential energy, and $\tilde{\delta} W$ are the vitual works of forces, which can not be derived by gradient calculation from a potential.

For the r-dependence of the disk deflections v_{wd}, u_{wdr}, u_{wdt} we choose the following shape function, i.e. polynomials in r (R_{wdi} is the inner radius of the wheel disk):

$$(2.2) \qquad u_{wdt}(r, \varphi, t) = a_{t1}(\varphi, t)(r/R_{wdi} - 1) + a_{t2}(\varphi, t)(r/R_{wdi} - 1)^2 \ ,$$

$$(2.3) \qquad u_{wdr}(r, \varphi, t) = a_{r1}(\varphi, t)(r/R_{wdi} - 1) + a_{r2}(\varphi, t)(r/R_{wdi} - 1)^2 \ ,$$

$$(2.4) \qquad v_{wd}(r, \varphi, t) = a_{v1}(\varphi, t)(r/R_{wdi} - 1)^2 + a_{v2}(\varphi, t)(r/R_{wdi} - 1)^3 \ .$$

Since the disk is clamped at the hub, the shape function for v_{wd} has no constant or linear terms in $(r/R_{wdi} - 1)$.

Putting these functions in (2.1) one obtains, after partial integration with respect to time and the space variables, the partial differential equations for the continuous parts of the system, the ordinary differential equations for the hub (rigid body) and the mechanical boundary conditions. After transformation of the material coordinate φ to $\psi := \varphi - \Omega t + \beta_{wh} - \beta_{wc}$ ($\mathbf{v}_{wd} = (a_{v1}, a_{v2})^T$, $\mathbf{u}_{wd} = (a_{r1}, a_{r2}, a_{t1}, a_{t2}, \beta_{wr})$, β_{wc} determines the point of contact on the rim), the partial differential equations for the wheel disk and the rim are:

$$(2.5) \qquad 0 = D_{wp}[\mathbf{v}_{wd}] + \mathbf{g}_{wpv}\ddot{v}_{wh} + \sin(\psi)(\dot{\alpha}_{wh}\mathbf{g}_{wp\alpha1} + \ddot{\gamma}_{wh}\mathbf{g}_{wp\gamma2})$$
$$+ \cos(\psi)(\ddot{\alpha}_{wh}\mathbf{g}_{wp\alpha2} + \dot{\gamma}_{wh}\mathbf{g}_{wp\gamma1}) \ ,$$

$$(2.6) \qquad 0 = D_{ws}[\mathbf{u}_{wd}] + \mathbf{g}_{ws\beta1}\dot{\beta}_{wh} + \mathbf{g}_{ws\beta2}\ddot{\beta}_{wh} + \sin(\psi)(\dot{u}_{wh}\mathbf{g}_{wsu1}$$
$$+ \ddot{u}_{wh}\mathbf{g}_{wsu2} + \dot{w}_{wh}\mathbf{g}_{wsw1} + \ddot{w}_{wh}\mathbf{g}_{wsw2}) + \cos(\psi)(\dot{u}_{wh}\mathbf{g}_{wsu3}$$
$$+ \ddot{u}_{wh}\mathbf{g}_{wsu4} + \dot{w}_{wh}\mathbf{g}_{wsw3} + \ddot{w}_{wh}\mathbf{g}_{wsw4}) \ .$$

Here D_{wp} and D_{ws} are linear differential operators (differentiation with respect to ψ and t). With respect to ψ, D_{wp} is of fifth order and D_{ws} is of third order, with respect to t they are of second order. The order with respect to ψ is by one higher than the order of the Kirchhoff plate theory or the shell theory, respectively, because material damping and the moving coordinate ψ raises the order (cf. MEYWERK [3]). The tuples $\mathbf{g}_{wp..}$ have five elements, the tuples $\mathbf{g}_{ws..}$ have two elements. The coupling terms between the hub deflections and rotations on the one side and plate and shell deflections on the other side, result from the terms in the kinetic energy. Thus, these tuples depend on the geometry and on the mass densities. Elastic constants occur in D_{wp} and D_{ws} only.

We restrict the linearized ordinary differential equations for the hub to those for v_{wh}, α_{wh}, and u_{wh}. The remaining three equations look similar:

$$(2.7) \qquad 0 = m_w \ddot{v}_{wh} + b_{whv} \dot{v}_{wh} + k_{whv} v_{wh}$$

$$+ \int\limits_{\psi=0}^{2\pi} \mathbf{g}_{whv}^T (\ddot{\mathbf{v}}_{wd} - 2\Omega \dot{\mathbf{v}}'_{wd} + \Omega^2 \mathbf{v}''_{wd})\, \mathrm{d}\psi + F_{c2} + F_{wa2}\,,$$

$$(2.8) \qquad 0 = J_{w1} \ddot{\alpha}_{wh} + \Omega J_{w2} \dot{\gamma}_{wh} + b_{whw}(b_{ws}^2 \dot{\alpha}_{wh} + b_{ws} \dot{w}_{wh})$$

$$+ k_{whw}(b_{ws}^2 \alpha_{wh} + b_{ws} w_{wh}) + \int\limits_{\psi=0}^{2\pi} \Big\{ \sin(\psi)[\mathbf{g}_{wh\alpha 1}^T (\dot{\mathbf{v}}_{wd} - \Omega \mathbf{v}'_{wd})$$

$$+ \mathbf{g}_{wh\alpha 2}^T (\ddot{\mathbf{v}}'_{wd} - \Omega \dot{\mathbf{v}}''_{wd} + \mathbf{v}'''_{wd}) + \mathbf{g}_{wh\alpha 3}^T \mathbf{v}'_{wd}] + \cos(\psi)[\mathbf{g}_{wh\alpha 4}^T \mathbf{v}_{wd}$$

$$+ \mathbf{g}_{wh\alpha 5}^T (\dot{\mathbf{v}}'_{wd} - \Omega \mathbf{v}''_{wd}) + \mathbf{g}_{wh\alpha 6}^T (\ddot{\mathbf{v}}_{wd} - \Omega \dot{\mathbf{v}}'_{wd} + \mathbf{v}''_{wd})] \Big\}\, \mathrm{d}\psi + F_{c2}(R_{wdo}$$

$$+ \tilde{h}_{wr}(0)) + M_{wa1} + P(-\alpha_{wh}(R_{wdo} + \tilde{h}_{wr}(0)) + v_{cw} + g_c(\mathbf{v}_{wd}))\,,$$

$$(2.9) \qquad 0 = m_w \ddot{u}_{wh} + b_{whu}(\dot{u}_{wh} - b_{ws} \dot{\gamma}_{wh}) + k_{whu}(u_{wh} - b_{ws} \gamma_{wh})$$

$$+ F_{c1} + F_{wa1} + \int\limits_{\psi=0}^{2\pi} \Big\{ \sin(\psi)[\mathbf{g}_{whu1}^T \mathbf{u}_{wd} + \mathbf{g}_{whu2}^T (\dot{\mathbf{u}}_{wd} - \Omega \mathbf{u}'_{wd})$$

$$+ \mathbf{g}_{whu3}^T (\ddot{\mathbf{u}}_{wd} - \Omega \dot{\mathbf{u}}'_{wd} + \mathbf{u}''_{wd})] + \cos(\psi)[\mathbf{g}_{whu4}^T \mathbf{u}_{wd}$$

$$+ \mathbf{g}_{whu5}^T (\dot{\mathbf{u}}_{wd} - \Omega \mathbf{u}'_{wd}) + \mathbf{g}_{whu6}^T (\ddot{\mathbf{u}}_{wd} - \Omega \dot{\mathbf{u}}'_{wd} + \mathbf{u}''_{wd})] \Big\}\, \mathrm{d}\psi\,.$$

Here m_w is the mass of the whole wheel, $b_{wh.}$, $k_{wh.}$ ($\cdot$ stands for u, v, w) are the damping or stiffness, resp., of the primary suspension of the wheel, i.e. the

connection between the hub and the wheel frame. The moments of inertia are J_{wi} ($i = 1,2$) and the distance between the centre of mass of the hub and the primary suspension is b_{ws}. The contact forces are denoted by F_{ci} and the forces and moments between the axle and the hub by F_{wai} ($i = 1,2,3$) and M_{wa1}. The tuples $g_{wh..}$ are due to the coupling between the hub and the disk. Furthermore, R_{wdo} is the outer radius of the wheel disk, $\tilde{h}_{wr}(\psi)$ is the height of the rim in dependence on the coordinate ψ. This means, that $\tilde{h}_{wr}(0)$ is the height of the rim at the point of contact. The static load P represents the weight of the coach, g_c is a linear differential operator, and v_{cw} is the displacement of the point of contact in the $\vec{e}_{g2}$-direction. The expression with the load P takes into account the moment which acts if the point of contact does not lie in the direction of P. The mechanical boundary conditions are:

$$(2.10) \qquad (0,0)^T = [B_{wp1}[\mathbf{v}_{wd}]]_{0+}^{2\pi^-} + F_{c2}\mathbf{b}_{wp1}^T + P\mathbf{b}_{wp2}(\mathbf{v}_{wd})$$

$$(0,0)^T = [B_{wp2}[\mathbf{v}_{wd}]]_{0+}^{2\pi^-} + M_c\mathbf{b}_{wp3}^T,$$

$$(2.11) \qquad (0,0,0,0,0)^T = [B_{wp3}[\mathbf{u}_{wd}]]_{0+}^{2\pi^-} + F_{c1}\mathbf{b}_{wp4}^T\delta + F_{c3}\mathbf{b}_{wp5}^T + P\mathbf{b}_{wp6}(\mathbf{u}_{wd}) ,$$

$$(2.12) \qquad (0,0)^T = [\mathbf{v}_{wd}]_{0+}^{2\pi^-} ,$$

$$(2.13) \qquad (0,0)^T = [\mathbf{v}'_{wd}]_{0+}^{2\pi^-} ,$$

$$(2.14) \qquad (0,0,0,0,0)^T = [\mathbf{u}_{wd}]_{0+}^{2\pi^-} .$$

Here B_{wp1}, B_{wp2}, and B_{wp3} are linear differential operators with respect to ψ and t (the time derivatives in the boundary conditions are due to the moving coordinate ψ and the material damping). With respect to ψ, they have the order of four (B_{wp1}), three (B_{wp2}), and two (B_{wp3}), and with respect to t they have the order of one. The tuples $\mathbf{b}_{wpi}$ ($i = 1, \ldots, 6$) depend on the geometry. Furthermore, $\mathbf{b}_{wp1}$, $\mathbf{b}_{wp2}$, $\mathbf{b}_{wp4}$, and $\mathbf{b}_{wp6}$ depend on $\tilde{h}_{wr}(0)$ and $\mathbf{b}_{wp2}$ and $\mathbf{b}_{wp6}$ are a linear function of $\mathbf{v}_{wd}$ and $\mathbf{u}_{wd}$, respectively. The notation $[\cdot]_{0+}^{2\pi^-}$ stands for $[f]_{0+}^{2\pi^-} :=$ $\lim\limits_{\psi \overset{\geq}{\to} 2\pi} f(\psi) - \lim\limits_{\psi \overset{\leq}{\to} 0} f(\psi)$.

The partial differential equations which govern the motion of the axle has been found by WAUER [11]:

$$(2.15) \qquad (0,0,0,0) = D_{wa1}[u_{wa}, w_{wa}, \alpha_{wa}, \gamma_{wa}] ,$$
$$(2.16) \qquad 0 = D_{wa2}[v_{wa}] ,$$
$$(2.17) \qquad 0 = D_{wa3}[\beta_{wa}] .$$

Here D_{wa1}, D_{wa2}, and D_{wa3} are linear partial differential operators with respect to y (of second order) and t (second order). The partial differential equations

(Timoshenko beam) for u_{wa}, γ_{wa} on one side and w_{wa}, α_{wa} on the other side, are coupled since the axle rotates; they would be decoupled for a vanishing angular velocity of the axle. Furthermore, the motions of the axle and the hubs are coupled by geometrical conditions. We give e.g. two coupling equations (for wheel 1), the other ten look similar (ℓ is the length of the axle and b_{wh} is the height of the hub in $\vec{e}_{g2}$-direction):

(2.18) $0 = u_{wa}(\ell) - u_{wh} + \gamma_{wh}b_{wh}/2,$ $0 = \gamma_{wa}(\ell) - \gamma_{wh}$.

For the shearing forces and moments F_{wai} and M_{wai} ($i = 1, 2, 3$) we give only two examples (for wheel 1), the other ten look again similar or are well known (EA_{wa} is the stiffness in extension and EI_{wa} in bending, η is the material damping parameter):

$$0 = F_{wa2} - EA_{wa}(v'_{wa}(\ell) + \eta\dot{v}'_{wa}(\ell)),$$

(2.19)

$$0 = M_{wa1} - EI_{wa}(\alpha'_{wa}(\ell) + \eta\dot{\alpha}'_{wa}(\ell) + \eta\Omega\gamma'_{wa}(\ell)) .$$

The partial differential equations for the rail read:

(2.20) $0 = D_{r1}[(u_r, \beta_r, w_r)] ,$

(2.21) $0 = D_{r2}[(v_r, \alpha_r, \gamma_r)] .$

Here D_{r1} and D_{r2} are linear differential operators with respect to s (of order three) and t (of order two). The movement of the coordinate $s = x - vt - u_{rc}$ and the material damping are the reasons for raising the order with respect to s; the reader would have expected order two because of the Timoshenko beam and the bar in torsion and extension. The partial differential equations for u_r on the one side and β_r, w_r on the other side are coupled because the Winkler foundation acts on the rail foot and because the centre of shear and the centre of mass of the rail cross-sections do not coincide. The same holds for the partial differential equation for α_r (torsion) and v_r, γ_r (Timoshenko beam). The mechanical boundary conditions at the point of contact are:

(2.22) $0 = F_{c1} + [B_{r1}[u_r]]_{0+}^{0-} ,$

$$0 = F_{c3} + [B_{r3}[w_r, \beta_r]]_{0+}^{0-} ,$$

$$0 = F_{c1}g_{r3} + Pg_{r4}(\beta_r) + [B_{r5}[\beta_r]]_{0+}^{0-} ,$$

$$0 = [u_r]_{0+}^{0-} ,$$

$$0 = [w_r]_{0+}^{0-} ,$$

(2.22)
[cont.]

$$0 = [\beta_r]_{0+}^{0-} ,$$

$$0 = F_{c2} + [B_{r2}[v_r, \gamma_r]]_{0+}^{0-} ,$$

$$0 = F_{c2}g_{r1} + Pg_{r2}(\alpha_r) + [B_{r4}[\alpha_r]]_{0+}^{0-} ,$$

$$0 = M_c + [B_{r6}[\gamma_r]]_{0+}^{0-} ,$$

$$0 = [v_r]_{0+}^{0-} ,$$

$$0 = [\alpha_r]_{0+}^{0-} ,$$

$$0 = [\gamma_r]_{0+}^{0-} .$$

Here B_{ri} $(i = 1, \ldots 6)$ are linear differential operators with respect to s (order two) and t (order one) and g_{ri} $(i = 1, \ldots, 4)$ depend on geometric parameters and stiffnesses.

The contact equations can be summarized in the following form:

$$(2.23) \quad (0, 0, F_{c3})^T = g_{cr1}(u_r, v_r, w_r, \alpha_r, \beta_r, \gamma_r)|_{s=0}$$

$$-g_{cw1}(\tilde{h}_{wr}, u_{wh}, v_{wh}, w_{wh}, \alpha_{wh}, \beta_{wh}, \gamma_{wh}, \mathbf{v}_{wd}, \mathbf{u}_{wd})|_{\psi=0} ,$$

$$(2.24) \quad (0, 0)^T = D_{cr1}[u_r, v_r, w_r, \alpha_r, \beta_r, \gamma_r]|_{s=0} - D_{cw1}[\partial\tilde{h}_{wr}/\partial\psi,$$

$$m u_{wh}, v_{wh}, w_{wh}, \alpha_{wh}, \beta_{wh}, \gamma_{wh}, \mathbf{v}_{wd}, \mathbf{u}_{wd}]|_{\psi=0} ,$$

$$(2.25) \quad (\nu_1, \nu_2, \Phi_c)^T = D_{cr2}[u_r, v_r, w_r, \alpha_r, \beta_r, \gamma_r]|_{s=0}$$

$$- D_{cw2}[u_{wh}, v_{wh}, w_{wh}, \alpha_{wh}, \beta_{wh}, \gamma_{wh}, \mathbf{v}_{wd}, \mathbf{u}_{wd}]|_{\psi=0} ,$$

$$(2.26) \quad \begin{pmatrix} F_{c1} \\ F_{c2} \\ M_c \end{pmatrix} = Ga_{ce}b_{ce} \begin{pmatrix} c_{11} & 0 & 0 \\ 0 & c_{22} & \sqrt{a_{ce}b_{ce}}c_{23} \\ 0 & -\sqrt{a_{ce}b_{ce}}c_{23} & a_{ce}b_{ce}c_{33} \end{pmatrix} \begin{pmatrix} \nu_1 \\ \nu_2 \\ \Phi_c \end{pmatrix} .$$

Here g_{cr1} and g_{cw1} are linear functions. The first two equations of (2.23) ensure that the wheel and the rail do not loose contact. The third equation of (2.23) is the linearized Hertzian contact equation. The operators D_{cr1} and D_{cw1} are linear differential operators with respect to s and ψ, respectively. Equations (2.24) ensure that the tangential planes of the wheel and the rail in the point of contact are parallel. The operators D_{cr2} and D_{cw2} are linear differential operators with respect to s and ψ (order one), respectively, and with respect to t (order one). Here ν_1 and ν_2 are the slips, i.e. the relative velocities in the point of contact between the wheel and rail divided by v, and Φ_c is the spin. These quantities enter

the equation of Kalker's linear theory (2.26). In (2.26) G is the shear modulus, a_{ce} and b_{ce} are the radii of the contact ellipse, and c_{11}, c_{22}, c_{23}, and c_{33} are Kalker's coefficients.

From Hertz's and Kalker's theory it is known, that the constants a_{ce}, b_{ce} and Kalker's coefficients in (2.26) fluctuate, i.e. they are not constant. For example, the radii of the contact ellipse depend on the normal force and on the mutual wheel rail position. Furthermore, Kalker's coefficients depend on these parameters, too. We assume in our approach first, that the rail surface is an ideal cylinder and the wheel surface is an ideal cone; second, that the changes of the mutual wheel-rail positions are small, i.e. we consider small oscillations only; and third, that the fluctuations in the normal force are small in comparison with the static load $P \approx 60$ kN, which is the mean value of the normal force. Assuming this, we can neglect the fluctuation in the radii and in Kalker's coefficients.

On the one hand, the model of the wheel set and the rail is very accurate but on the other hand, the foundation of the rail is taken into account by a uniform Winkler foundation neglecting the periodic character. In the author's opinion, there are two reasons for the fact that the periodic foundation do not influence the rumbling noise:

1. If the periodic foundation would cause the rumbling noise, then the noise must occur frequently. But it is known from experience that noise in the ICE trains occurs if the wheels are out-of-round and the noise vanishes if the wheels are round.

2. If the periodic foundation would cause the rumbling, there must be a peak in the spectrum which has to fit the periodic excitation of the foundation. In MÜLLER-BORUTTAU and EBERSBACH [7] the spectrum of the measured rumbling noise in an ICE train (velocity 260 km/h $\approx$ 72.22 m/s, radius of the wheels $R = 0.46$ m, sleeper distance 0.6 m) is published. In the frequency range from 20 Hz to 130 Hz there occur six peaks: 25 Hz (95 dB), 100 Hz (95 dB), 50 Hz (92 dB), 75 Hz (87 dB), 125 Hz (82 dB), 120 Hz (80 dB). The values in brackets denote the heights of the peaks. The first five peaks result from the out-of-round wheel (the frequencies are multiples of $(72.22\,\text{m/s})/(2\pi\,0.46\,\text{m}) \approx 24.99$ Hz). The smallest peak at 120 Hz is the result of the periodic foundation $((72.22\,\text{m/s})/0.6\,\text{m} \approx 120.4\text{Hz})$. Thus, the smallest peak at 120 Hz can not be the reason of the rumbling. It seems to be admissible to neglect the periodic foundation.

We assume that the non-circular profiles of the wheels can be expanded into Fourier series with a finite number of non-zero Fourier coefficients. The non-circularities are described by φ-dependent heights of the rims; for one rim we have:

$$(2.27) \qquad h_{wr}(\varphi) = h_{wr0} + \sum_{\substack{n=-N \\ n \neq 0}}^{N} C_{wrn} e^{jn\varphi} \, ,$$

where C_{wrn} are the complex Fourier coefficients; the coefficient C_{wrn} is the complex conjugate of $C_{wr(-n)}$. Since the model is linear, the forced oscillations caused by a single term $C_{wrn}e^{jn\varphi}$ of the Fourier series can be calculated and the superposition of all terms yields the oscillations of the system. In the following we sketch how the oscillations caused by a single term are calculated, i.e. how the solution of the set of governing equations is determined.

For this harmonic excitation we write $u_r = \hat{u}_r e^{j\omega t}$ ($\omega = n\Omega$, Ω is the mean angular velocity of the wheel set, j is the imaginary unit) and we consider this excitation as the right-hand side. First we separate the time dependence $e^{j\omega t}$. As a result, the partial differential equations which describe the one-dimensional continua rails and axle are simplified to ordinary differential equations with respect to the spatial variables s or y, respectively, which are fulfilled by an $e^{\kappa_r s}$- or an $e^{\kappa_{wa} y}$-ansatz. This approach leads to standard eigenvalue problems for the eigenvalues κ_r and κ_{wa}, which are solved numerically. To solve the partial differential equations of the wheel disks, we separate the variables φ and r and choose a polynomial in r for the r-dependence and an $e^{\kappa_w \varphi}$-ansatz for the φ-dependence. This procedure results in a standard eigenvalue problem for the eigenvalue κ_w. It is solved numerically, too. The numerically calculated solutions of the eigenvalue problems are substituted into the contact equations which leads to a set of linear algebraic equations. The coefficients are comprised in a matrix $\mathbf{M}(\omega)$. We obtain the forced vibration of the system by inversion of the matrix $\mathbf{M}(\omega)$ and multiplying the inverse by $\hat{u}_r$. Since we assume the model to be asymptotically stable (in the sense of Ljapunow), the inverse $\mathbf{M}^{-1}(\omega)$ exists. One can find a detailed description of the procedure of solution in MEYWERK and BROMMUNDT [5] or MEYWERK [4].

In the following we sketch how the non-circular wheels force the system to oscillate. We start with the terms of excitation (the above mentioned right-hand-side-terms $u_r = \hat{u}_r e^{j\omega t}$) and concentrate on the terms caused by one wheel; the calculation for the second one has to be done in the same way. One excitation term is due to the vertical contact force F_{c3} between wheel 1 and rail 1. It is:

$$(2.28) \qquad F_{c3} = P + k_H \underbrace{\left(f_w - f_r + \tilde{h}_{wr} - h_{wr0} \right)}_{:=\Delta f} .$$

Here k_H is the linearized Hertzian contact stiffness and P is the static load caused by the weight of the coach. The sum Δf comprises the time-dependent elastic flattening of the wheel and the rail in the contact area. This flattening depends on the deflections and deformations of the wheel set ($u_{wa}, v_{wa}, w_{wa}, \alpha_{wa}\ \beta_{wa}, \gamma_{wa}, u_{wh}, v_{wh}, w_{wh}, \alpha_{wh}, \beta_{wh}, \gamma_{wh}, v_{wd}, u_{wdr}, u_{wdt}$, abbreviated by f_w), the rail ($u_r, v_r, w_r, \alpha_r, \beta_r, \gamma_r$, abbreviated by f_r), and on the difference between the mean value of the height of the rim h_{wr0} and the height $\tilde{h}_{wr}$ of the non-circular wheel rim

at the point of contact. Another excitation is due to the geometrical requirement that the tangential planes of the wheel and the rail should be parallel.

The height of the rim at the point of contact $\tilde{h}_{wr}$, which enters Eq. (2.28), is in linear approximation $\tilde{h}_{wr} = h_{wr}(\Omega t)$, where Ω is the mean value of the angular velocity of the wheel set. We have

$$
F_{c3} = P + k_H \left(f_w - f_r + \underbrace{\sum_{\substack{n=-N \\ n\neq 0}}^{N} C_{wrn}e^{jn\Omega t}}_{\text{right-hand sides}} \right) ,
$$

where we can identify the right-hand side excitation terms.

3. NUMERICAL RESULTS

Measurements show that the rumbling is caused by non-circular wheels, i.e. rumbling can only be observed if the wheels are non-circular. The measured Fourier decomposition of the non-circularities of the wheels show that the absolute values of the Fourier coefficients have a maximum around the coefficient of the fifth harmonic (cf. MÜLLER and DIENER [6]).

For a better understanding of the growth of rumbling, it is helpful to look at the eigenvalues and the corresponding natural modes of the system. In Fig. 6 the eigenvalues of the system up to 150 Hz are depicted; the foundation is as stiff as it is at the new tracks of DB. We focus on the eigenvalues λ_4 and λ_5 which play the essential role in the growth of rumbling. First of all we have a look at the natural modes, which are depicted in Fig. 7 and Fig. 8. In these figures the undeformed wheel set and the undeformed tracks are outlined using thin circles or lines. The deformed ones are depicted by bold lines. To get a better impression of the deformation of the different parts, the deformed and the undeformed wheels, rails, and axle are joined by lines. The modes describe vertical oscillations of the wheels and the rails; in Fig. 7 the right and the left wheel-rail-pair oscillate in phase and in Fig. 8 in antiphase. These eigenmodes are mainly excited by non-circular wheels if the Fourier decomposition of the non-circularities contain the fourth, the fifth or the sixth harmonic and the velocity is approximately 60 m/s–70 m/s. Trains with such non-circular wheels travel both on new, stiff and on old, soft tracks, and the eigenmodes exist both on the new and old tracks.
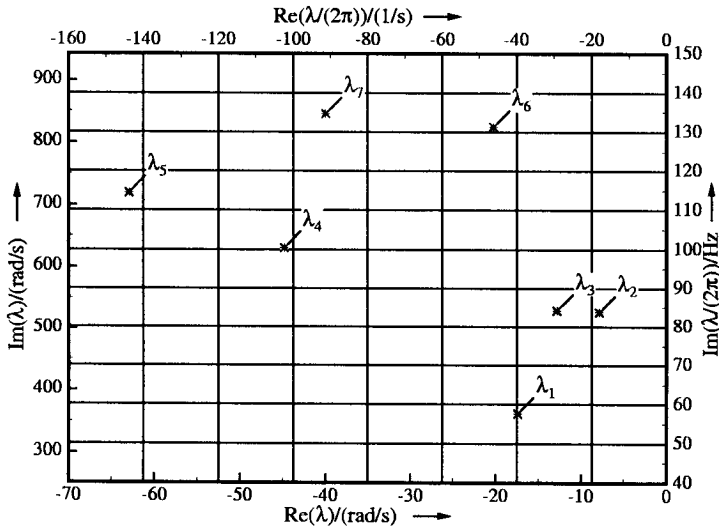
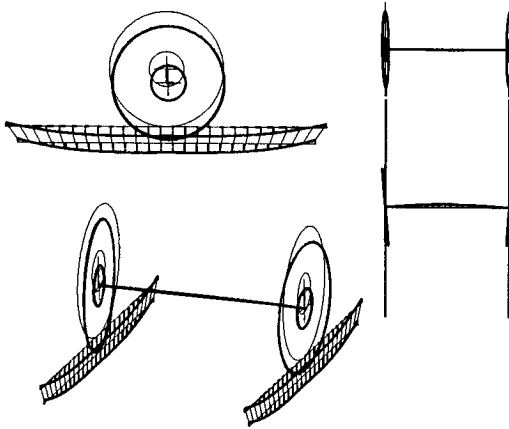FIG. 6. The eigenvalues up to 150 Hz.

FIG. 7. The natural mode to the eigenvalue $\lambda_4 = (-44.7 + j630.5)/s$.

Therefore, three questions arise:

1. Why does the rumbling occur on the new stiff tracks independently of the velocity of the trains?

2. Why does the rumbling not occur as often on the old tracks as it does on the new ones?

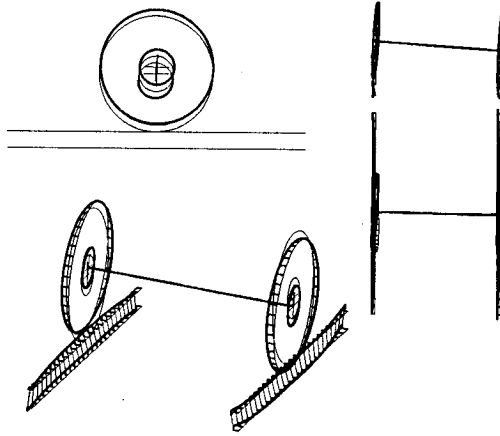3. Why is the rumbling more noisy on the new tracks than it is on the older ones?

FIG. 8. The natural mode to the eigenvalue $\lambda_5 = (-62.8 + j719.0)/s$.

To answer the questions, we first look at the change of the eigenvalues λ_1, λ_2, λ_3, λ_4, λ_5 if the vertical track stiffness k_{rw} and damping b_{rw} increases. The values k_{rw} and b_{rw} are the parameters of a Winkler foundation, i.e. the force per length in vertical direction, which is due to the foundation, is $b_{rw}\dot{w}_r + k_{rw}w_r$. The imaginary parts of the eigenvalues for the variation of k_{rw} and b_{rw} are depicted in Fig. 9. For the soft tracks one can see that the imaginary parts of those eigenvalues, which belong to the mainly vertical oscillations, are close together and at low frequencies (about 70 Hz). For the stiffer tracks the imaginary parts diverge and the frequencies increase (about 110 Hz). The small distance between the eigenvalues for the soft track and a larger distance for the stiffer track answer the first and the second question: A small distance between the eigenvalues causes a narrow resonance peak. For high vertical forces and loud rumbling it is necessary that the excitation from the wheels should fit the resonance peak. Therefore, the rumbling occurs in small velocity intervals only, i. e. in those velocity intervals in which the excitation frequency fits the resonance peak. A larger distance between the eigenvalues for the stiff tracks causes a wider peak. This raises the probability, that the frequency caused either by the fourth, the fifth, or by the sixth harmonic, fits the resonance peak. This means that an excitation frequency exists which fits the peak nearly independently of the velocity.

Higher frequencies of the mainly vertical oscillations (eigenmodes λ_4 and λ_5) partially answer the question three: The damper between bogie and coach (the so-called secondary suspension) is stiffer for higher frequencies. Thus, the oscillations of the wheel sets on the new stiffer tracks are not as well isolated from the coaches as on the softer tracks. But there is another reason for the noisy rumbling on the stiff tracks. We explain this reason with the help of Fig. 10. We
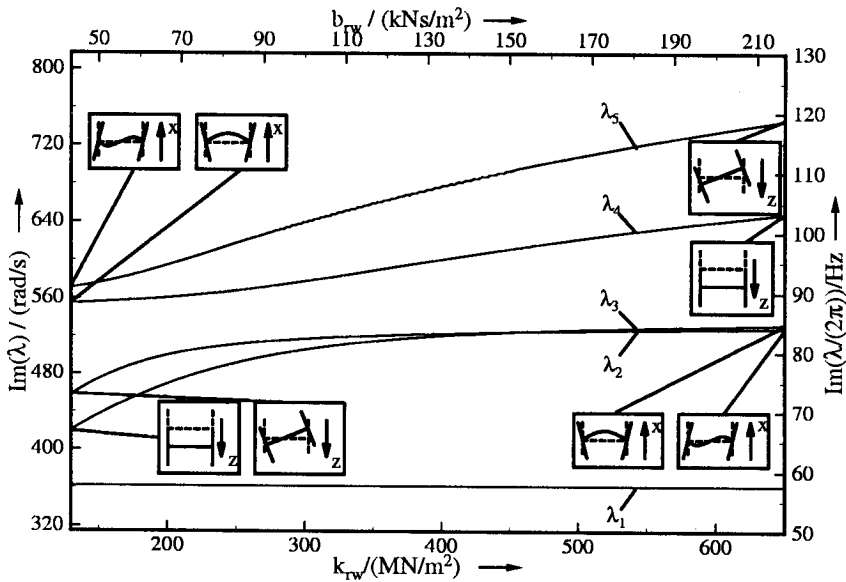
FIG. 9. Imaginary parts of the eigenvalues λ_1, λ_2, λ_3, λ_4, λ_5 as functions of the vertical stiffness parameters k_{rw}, b_{rw}.
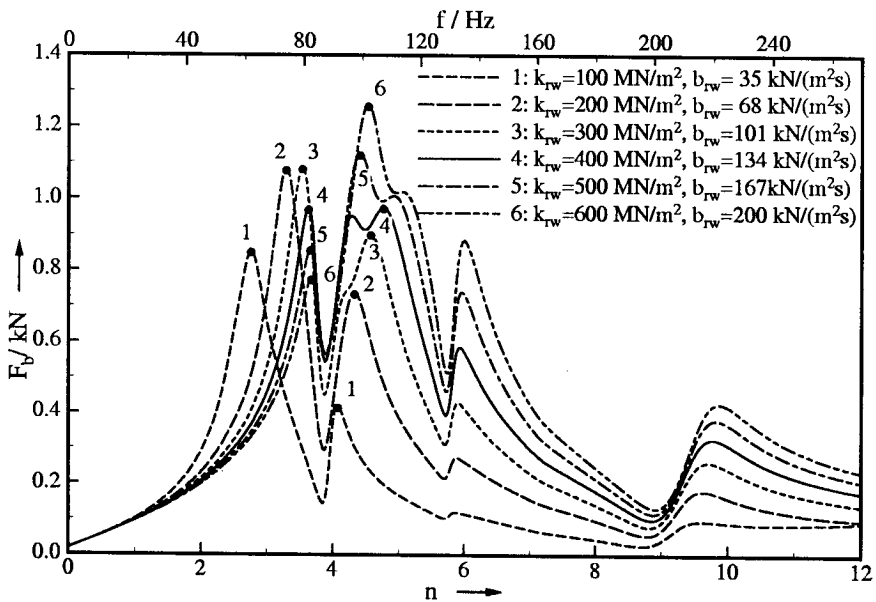

FIG. 10. Vertical force F_b as a function of the order of the Fourier expansion for different foundation parameters.

[329]

investigate a wheel set with a non-circular wheel 1 and choose the height h_{wr} of the rim of wheel 1 to be:

$$h_{wr} = 20 \, \mu\text{m} \cos(n\varphi) \,,$$

where n is a natural number. This results in an excitation frequency of $\omega = n\Omega$. For this wheel set, the force $\tilde{F}_b = F_b \cos(n\Omega + \alpha_s)$ (α_s phase shift) between the bogie and primary suspension is calculated; in Fig. 10 the amplitudes F_b are shown. To obtain the resonance curves, the number n is varied continuously. Of course, the values of F_b for non-natural numbers are artificial, but they make sense for other velocities. The resonance peaks for the soft track (curve 1) and the stiff track (curve 5) differ in their height and width: The peak for the stiff track is higher and wider than the peak of the soft track. The consequences of the wider peak at a higher frequency have been discussed above. The height of the peak, which is larger for the stiff track than it is for the softer ones, increases the rumbling, additionally to the increase caused by the stiffer secondary suspension.

4. Conclusions

Some hints concerning the reasons of the rumbling in the high-speed train ICE of the DB are given. The resonance of two mainly vertical oscillating eigenmodes play the main part in the growth of rumbling. These eigenmodes are excited by non-circular wheels. The divergence and the increase of the imaginary parts of the corresponding eigenvalues, and higher forces between wheel set and bogie are the reasons for the frequent occurrence of rumbling on the new stiff tracks. Nevertheless, the growth of the non-circularities of the wheels is not explained yet.

Acknowledgement

References

1. Y.C. Fung, *Foundations of solid mechanics*, Prentice-Hall International Series in Dynamics, Englewood Cliffs, N. J. Prentice-Hall, 1965.

2. J. J. Kalker, *Three-dimensional elastic bodies in rolling contact*, vol. 2 [in:] Solid Mechanics and its Application, Kluwer Academic Press, Doordrecht, 1990.

3. M. Meywerk, *Regularization in the governing equations of railway wheel models*, J. Theor. Appl. Mech. **34**, 1, pp. 31–42, 1996.

4. M. MEYWERK, *Stabilität und Verschleiß bei auf Schienen laufenden Eisenbahnradsätzen*, Bd. 30 aus: Braunschweiger Schriften zur Mechanik, Mechanik-Zentrum, TU Braunschweig 1997.

5. M. MEYWERK and E. BROMMUNDT, *Numerical investigation of the behaviour of a railroad wheel running on an infinite rail*, [in:] R. BOGACZ and K. POPP [Eds.], Dynamical problems in mechanical systems, Proceedings of the 3rd Polish–German Workshop, 26–31 July 1993 in Wierzba, 233–244, PAN, Warszawa.

6. R. MÜLLER and M. DIENNER, *Verschleisserscheinungen an Radlaufflächen von Eisenbahnfahrzeugen*, ZEV Glasers Ann. 119, 6, pp. 177–192, 1995.

7. F. H. MÜLLER-BORUTTAU and D. EBERSBACH, *Elastische Zwischenlagen im Gleis lösen Schwingungsprobleme*, [in:] H. HOCHBRUCK, K. KNOTHE and P. MEINKE [Eds.], Systemdynamik der Eisenbahn, pp. 87–95, Hestra–Verlag, Darmstadt, 1994.

8. W. D. PILKEY, *Formulas for stress, strain, and structural matrices*, John Wiley and Sons, New York 1994.

9. D. TEICHMANN, *Schwingungen von Kreisringbalken*, Z. Angew. Math. Mech. 60, T81-T84, 1980.

10. K. WASHIZU, *Variational methods in elasticity and plasticity* (2. Ed.), 9 aus: International Series of Monographs in Aeronauticcs and Astronautics, Oxford: Pergamon Press.

11. J. WAUER, *Stabilität viskoelastischer Wellen unter axialem Druck*, Z. Angew. Math. Mech. 65(8), 379–380, 1985.

TECHNISCHE UNIVERSITÄT BRAUNSCHWEIG
INSTITUT FÜR TECHNISCHE MECHANIK,

Postfach 3329, 38023 Braunschweig